C_{60}/Zeolite Semiconductor Electrode and the Gas Sensing

Katsumi Tanaka,*,†,‡ Cheow-Keong Choo,† Seiji Sumi,‡ Yoshiyuki Kamitani,§ Toshiyuki Fujii,§ Kyouko Satoh,‡ Kei-ichiro Fukuda,‡ and Rhouhei Nakata†,‡

Department of Human Communication, The University of Electro-Communications, 1-5-1 Chufugaoka, Chofu Tokyo 182-8585, Japan, Graduate School of Electronic Engineering, The University of Electro-Communications, 1-5-1 Chufugaoka, Chofu Tokyo 182-8585, Japan, and Department of Electronic Engineering, The University of Electro-Communications, 1-5-1 Chufugaoka, Chofu Tokyo 182-8585, Japan

Miki Yoshimune, Yusuke Yoshinaga, and Toshio Okuhara

Graduate School of Environmental Earth Science, Hokkaido University, Sapporo 060-0810, Japan

Received: December 18, 2001; In Final Form: February 20, 2002

Sodium Y type zeolite synthesized with homogeneous gels was deposited as thin films on tantalum tooth-combs type electrode. C_{60} molecules were deposited on the zeolite electrode surface by sublimation in a vacuum and were encapsulated in zeolite supercages by the thermal diffusion. The encapsulation was indicated by a decrease of the pore volume measured by argon gas adsorption. The potassium deposited K-C_{60}/zeolite electrode as well as zeolite and C_{60}/zeolite electrodes showed the behaviors characteristic to semiconductors in their measurements of currents in dark with temperature. The dependence of their dark currents on temperature was similar, which suggests that carrier formation through thermal band-gap excitation will be mainly caused by zeolite. The C_{60}/zeolite and K-C_{60}/zeolite electrodes showed rapid current responses repeatedly at 298 K under UV light irradiation. The introduction of oxygen gas to the C_{60}/zeolite electrode under UV light irradiation resulted in both rapid and slow current decays with time. The current decreased and that remained in the rapid current decay were interpreted as contributions mainly from n-type (80%) and p-type character (20%), respectively. The slow current decay was interpreted by diffusion of oxygen into zeolite supercages. Ethylene sensing on the C_{60}/zeolite electrode was possible in dark and showed a pressure dependency of Langmuir type isotherm. The result implies that such sensing is caused by compressing ethylene molecules in zeolite supercages.

Introduction

Since the discovery in 1985,[1] carbon C_{60} fullerene has gathered much interest. The presence of superconducting transition temperature in alkali-intercalated fullerenes[2−4] has raised a number of studies on the transport properties.[5−7] The electronic properties have been associated with the structure of solid state, however there are many unsolved phenomena on diffusion of gases.[8] Whereas fullerenes have never succeeded to show champion data in any field, still have revealed attractive characteristics in many fields for the applications. The discovery of icosahedral symmetry structure[9] has led to an explosion in synthetic chemistry, especially the application to inclusion chemistry and the synthesis of fullerene derivatives. For instance, a water soluble fullerene was synthesized by embedding C_{60} in γ-cyclodextrin.[10] Lipophilic fullerene derivatives with long alkyl chains attached have been synthesized to obtain high solubility in bilayers, which enlarges the wide range of applications for bilayer membranes, especially with biocompatible functions,[11,12] while fullerene C_{60} molecules forms intramolecular and intermolecular charge-transfer (CT) complexes with tertiary amines[13,14] and aromatic rings.[15,16] High photogeneration efficiency of CT complexes has been observed in arylamine and C_{60} system.[17] Recently high stable C_{60}/poly(vinylpyrrolidone) CT complexes have been used for biological applications in water.[18] C_{60} incorporated nanocomposite systems also show improved resist performances for lithography.[19,20] It is the outstanding advantage in the device technology that fullerene molecules in resist can be completely removed by oxygen plasma.

In the meanwhile, the inclusion chemistry has been applied to C_{60}/zeolite systems. Zeolites are inorganic silicate materials composed of sodalite cages, which make up different sizes of three-dimensional pore structures. There are many types of zeolites with different alignments of sodalite cages and supercages and as a result with different pore sizes.[21] An ESR study shows that C_{60} molecule is trapped as C_{60}^{a} in X-type faujasite zeolite, suggesting that pairs of C_{60}^{-} ions are present in supercages.[22] Another ESR work studies the interaction between C_{60} molecules and zeolites and found C_{60}^{+} cation radicals at the entrances to supercages in HY zeolite.[23] It is assumed that C_{60} is not embedded in zeolite supercages in the latter paper, while it is concluded that C_{60} is embedded in zeolite suspercages from thermogravimetric analysis.[24] C_{60} can be also confined in one-dimensional channels of VFI (VPI-5) zeolite.[25] The advantage of the system is that white light can be observed in confined C_{60} molecules, even at 298 K; although, emission intensity from C_{60} itself is suppressed considerably at 298 K.[26] Recently, a one-dimensional channel of AFI ($AlPO_4$-5) has been signifi-

* To whom all correspondence should be addressed. E-mail address: tanaka@hc.uec.ac.jp.
† Department of Human Communication.
‡ Graduate School of Electronic Engineering.
§ Department of Electronic Engineering.

10.1021/jp014554f CCC: $22.00
Published on Web 04/02/2002

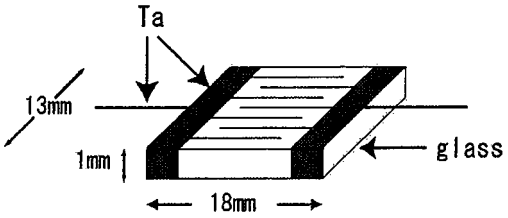

Figure 1. Schematics of tooth-comb type electrodes used, in which numbers of wires are not correct, shown for simplicity. Tantalum wires are spot-welded with Ta films with 2 mm distance and are supported on a glass substrate. Two such electrodes are placed in 1 mm distance as shown.

cantly applied to carbon nanotube synthesis.[27] The innersurface of these zeolites is very inert because no hydroxyl group exists. As a result it is difficult to make strong chemical bond with functional groups and species through OH group. Zeolite framework serves as electron pool for included species such as Si clusters to be stabilized as negatively charged state.[28] Since electron affinity of C_{60} is quite low (2.65 eV),[29] the inclusion in zeolite supercage will result in the anionic C_{60}^- state. C_{60} molecule is small enough to reach Y-type zeolite supercage through entrance of 12-membered ring with diamer of 0.74 nm: then the conductivity of C_{60}/zeolite should increase and the C_{60}/zeolite system can be studied as sensors for specific gases, the sizes of which are considered in comparison with the size of the zeolite supercage entrance. We succeeded in synthesizing zeolite, C_{60}/zeolite, and K-C_{60}/zeolite tooth-comb type electrodes. The following features about these electrodes are reported in this paper: (a) the semiconductor characteristics of the three electrodes, (b) the n- or p-type nature of a C_{60}/zeolite electrode determined using UV irradiation and oxygen gas adsorption, and (c) the gas sensing ability of the C_{60}/zeolite electrode.

Experimental Section

As shown in Figure 1, a tooth-comb was made with 0.1 mm diameter Ta wires, which were spot-welded on Ta film with distance of 2 mm. Two such Ta tooth-combs were placed physically face-to-face on the glass with a size of 13 mm × 18 mm × 1 mm (width × length × thickness). Consequently between two electrodes tooth-comb wires were placed at 1 mm distance. A gel for synthesizing faujasite NaY zeolite was prepared as that in ref 30. In the present study sodium metasilicate ($Na_2SiO_3 \cdot 9H_2O$), sodium aluminate ($Al_2O_3 \cdot 0.9Na_2O \cdot 0.84H_2O$), and silica ($SiO_2$) were added to water with the same molar ratio of 1:20:8:320 as that for Al_2O_3, SiO_2, NaO, and H_2O, and were mixed with stirring until they formed a homogeneous gel. The silica used was obtained by solvolysis of tetra-chlorosilane ($SiCl_4$) in water. The homogeneous gel was left overnight in water. The sensing unit was immersed in the gel, and the mixture was sealed in a Pyrex glass tube. The glass tube was heated at 368 ± 10 K for 150 h. NaY crystallines were synthesized and deposited on the sensing unit, which was washed with distilled water sufficiently. Hereafter the sensing unit, on which NaY zeolite film is deposited, is denoted as zeolite electrode. Figure 2 shows X-ray diffraction pattern of synthesized NaY zeolite in this study and that of commercially available NaY for comparison. Two patterns are quite identical. C_{60} with purity of 99.9%, commercially available, was used without further purification. C_{60} was thermally evaporated on the zeolite film deposited on the sensing unit, which was maintained at 573 K for thermal diffusion in the closed system maintained in oxygen free for about 1 week. C_{60} molecules

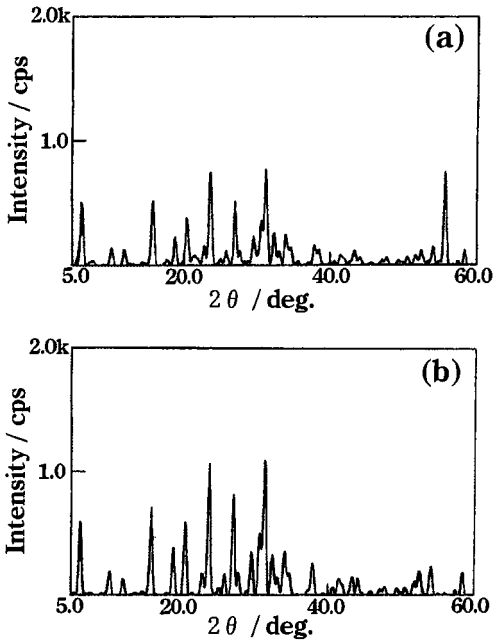

Figure 2. X-ray diffraction patterns of synthesized NaY zeolite (a) and commercially available one (b).

evaporated as the film on the zeolite film as well as on the sensing unit were removed by heating at 573 K under evacuation. It has been proved that the fullerene sublimation rate from the film is faster than the film deposition rate at temperatures above 573 K.[8] Hereafter the unit is denoted as the C_{60}/zeolite electrode.

Tiny amount of hydroxy groups was detected in the synthesized NaY zeolite after dehydration at 473 K with FT-IR spectrometer. For simplicity commercially available zeolites, HY-zeolite (JRC-Z-HY4.8) supplied from Catalyst Society of Japan and HY68-zeolite (Tosoh Corp. HSZ-320NAA) were used as standard zeolites to elucidate pore volume measured with argon adsorption experiments. BET surface areas of the former and the latter were 521 and 333 $m^2\ g^{-1}$, respectively. The ratios of Na^+ to H^+ exchange and of Si/Al in JRC-Z-HY4.8 and HSZ-320NAA were about 100%, 4.8 and 68%, 5.6, respectively. The complete ion exchange from Na^+ to H^+ in NaY zeolite will cause a structural deformation. The same treatment as in preparing the C_{60}/zeolite electrode was carried out to diffuse C_{60} into the pores of HY68 zeolite. Before argon adsorption began, the samples were evacuated at 473 K for 30 min to remove water. Argon adsorption was performed using an adsorption system (BELLSORP 28SA, BEL Japan, Inc.) at liquid argon temperature (87 K) in the range of the relative pressure (3×10^{-6}−10^{-1} of p/p_o). Micropore size distributions were calculated on the basis of argon isotherms with an area-averaged filled pore model.[31] The relation between the size of the micropores and relative pressure p/p_o, the relative pressure being determined at which time the pore is filled with argon, was derived theoretically.[31] The combination of the above relation with the isotherm (the volume of argon adsorbed vs the relative pressure) leads to a relation between the volume of adsorbed argon and the pore size. The micropore size distributions were expressed as the ratio of adsorbed volume change to pore size. Physical parameters for the argon adsorption and the computer program based on them were used as in the literature.[32]

Each electrode was placed horizontally parallel in specially designed Pyrex glass cell (3 cm diameter and about 30 cm length) whose end was connected to a 4-pin feed-through cone-

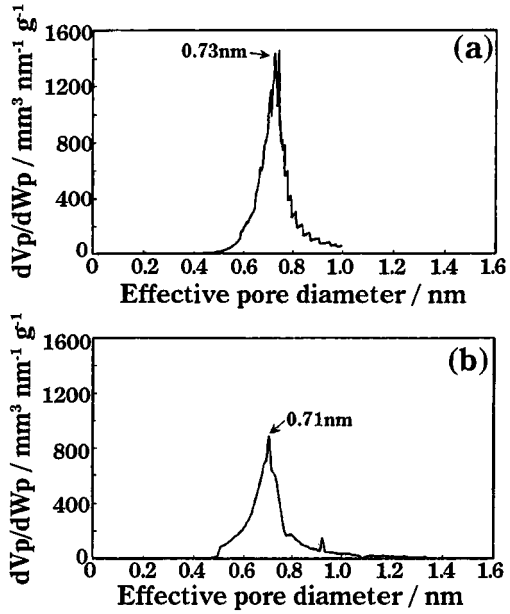

Figure 3. Pore size distributions of commercially available fresh Y-zeolite (a) and the one after thermal diffusion of C_{60} (b).

flat 70 flange. The connection of the feed-through to the glass cell was sealed for evacuation with Torr Seal (epoxy resin). The electrode surface was oriented face-down to the ground. The glass cell had a side tube whose end was finished with quartz window for UV irradiation. Current measurements were carried out at DC 5 V (50 V/cm) through the 4-pin feed-through flange. The 2 pins were used for measuring current and the other 2 pins for measuring temperature with thermocouples. While measuring the current on the electrode, the latter 2 pins were open-circuited. Evacuation of the glass cell was performed with a rotary-diffusion pump system through a greaseless glass stop valve attached to the cell. The electrode was heated indirectly by ribbon heater rounding outside the glass cell. Temperature difference between the electrode and glass was calibrated. Very weak current was measured with an electronic picoammeter (Takede Riken TR-8641); then all systems and cables were wrapped with aluminum foil for grounding. A deuterium lamp (Hamamatsu Photonics L1835, 150 W) irradiated the electrode at a 45° angle to the surface normal through the quartz window. Ethylene gas was purified by several freeze−pump−thaw cycles. Oxygen gas was purified by removing water after passing through molecular sieve trap maintained at 77 K. Gas adsorption experiments were carried out at 298 K. The C_{60}/zeolite electrode was evacuated at 573 K for 30 min before current measurements. Potassium metal was transferred from a bottle filled in oil to the current measuring cell with Schlenk technique[33] using polystylene bag in nitrogen atmosphere. Potassium metal was cleaned with acetone to wash out organic solvent before transferring to the cell. The C_{60}/zeolite electrode was evacuated at 573 K then potassium was deposited on the electrode unit by thermal evaporation under vacuum. No further activation was carried out except for the evacuation at 298 K.

Results and Discussion

Figure 3 shows pore size distributions of fresh zeolite and C_{60} diffused zeolite, which were measured with argon adsorption experiments. In the fresh zeolite pore volume, typical in Y-type zeolite supercages at diameter of about 1.3 nm which can be measured with a diameter of 0.73 nm as windows for entrance is typical, but the volume is decreased in C_{60} diffused zeolite.

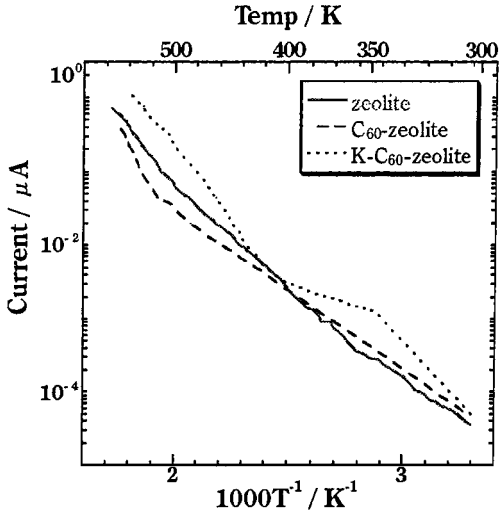

Figure 4. Currents under dark measured as a function of reciprocal to temperature on the zeolite, the C_{60}/zeolite and the K-C_{60}/zeolite electrodes represented in dotted, solid, and pointed lines, respectively.

Therefore it is clear that zeolite supercages are partially filled with C_{60} molecules in our thermal diffusion method. It will be interesting to estimate average fractional occupation of the supercages by C_{60} molecules. However, the result of Figure 3 implies an "apparent" pore volume occupation, which includes not only subsurface region but also bulk of zeolite pellet. C_{60} molecules should diffuse to zeolite supercages one by one from the deposited thin film through thermal diffusion. Then the supercages in the subsurface region will be occupied with C_{60} molecules. They should play a significant role on percolation paths for semiconductor behaviors mentioned in the next sections. How much C_{60} molecules can occupy one supercage of zeolite is quite significant to be studied in relation to the electronic conduction mechanism.

DC current in dark was measured on zeolite, C_{60}/zeolite, and K-C_{60}/zeolite electrodes as a function of temperature. As shown in Figure 4, currents are plotted in log scale. The horizontal scale is reciprocal of temperature represented in Kelvin. The logarithmically scaled DC current increased almost linearly with the reciprocal of temperature on three electrodes, that is, $(K_BT)^{-1}$. Here K_B is Boltzmann constant. Therefore it can be concluded that the three samples are semiconductors. The pristine oxygen-free C_{60} molecules show a high resistivity (about 10^{14} Ω cm).[34−36] The current on C_{60} will be too small to detect in normal instruments so that the observed currents on C_{60}/zeolite and K-C_{60}/zeolite electrodes will be related to zeolite electrode. It is quite significant that zeolite shows a semiconductor character. Zeolite framework is composed of $[SiO_4]^{4-}$ tetrahedra so that no current is expected. However, Na^+ ions as charge compensation to trivalent Al^{3+} ions situating positions of the lattice Si^{4+} ions will be mobile in addition to electron conductivity at elevated temperatures. Precisely speaking, the current vs $1/T$ dependence for pristine zeolite is not fairly linear. It will be reasonable to assume partially compensated semiconductor with both positive (Na^+) and negative (electrons and impurities) carriers. It is noted that an observed current is reflected by the number of C_{60}/zeolite-made circuit successfully (occasionally) bridging two tooth-comb electrodes, that is, the percolation path. Since the zeolite film is composed of μm-sized grains the detected current may be regulated by the conductance between the grains composed of C_{60}/zeolite composite. Therefore the vertical scale represents an apparent value and changes in each zeolite electrode. However, their

temperature dependency is reflected by the intrinsic nature. As each percolation path should show the same temperature dependency, it should be shown as the line with the same slope and the total number of percolation paths is represented as the respective vertical scale. In this study the current measurement was carried out on a zeolite film deposited electrode. Then C_{60} was diffused on the same zeolite electrode. Therefore the current of the C_{60}/zeolite electrode can be compared using the same zeolite electrode. Potassium was deposited on the same C_{60}/zeolite electrode. However, the current on the K-C_{60}/zeolite electrode increases drastically with the dosed amount of potassium. Although the amount of potassium was not defined, it was controlled to be quite small in order to see the temperature dependency of current in the same figure. The rurrent of K-C_{60}/zeolite in Figure 4 shows a unique temperature dependency. It showed much intense dependency than the other two electrodes from 300 to 350 K. The current became almost flat until 400 K and then increased again with the same dependency observed below 350 K. The influence of potassium diffusion into the C_{60}/zeolite electrode on the temperature dependence of current quite significantly impacts the discussion of the possibility of K_xC_{60} fostering cluster formation inside the pores and percolation between them. It should be studied more in detail. However, no more discussion is possible at this moment. Supposing that the dependency of dark current I on temperature can be expressed as follows, α increases in the order of C_{60}/zeolite, zeolite, and the K-C_{60}/zeolite electrode.

$$\log I = -\alpha(10^3/K_BT) + C \quad (1)$$

Conductivity depends both on density and mobility of electrons and/or holes. At the same time the density of carriers in log scale should depend linearly on $(K_BT)^{-1}$ at temperatures higher than 298 K (comparing to 0−300 K). In the so-called intrinsic region, the decline should reflect Eg/2. Here Eg shows the band gap. Supposing the same mobility and carriers for the three electrodes, their Eg values should increase in the same order as in α. It may be better to note that Eg values of C_{60}/zeolite and K-C_{60}/zeolite electrode are not so different from the Eg value of the zeolite electrode. If it is the case, it is suggested that the carrier formation through thermal band-gap excitation will mainly be brought about by zeolite electrode. As mentioned above, C in eq 1 is reflected by the number of percolation path between tooth-comb electrodes. At temperatures higher than about 523 K the nature of zeolite itself is responsible for the dark currents observed for the three electrodes.

The effect of UV irradiation on electrode current was studied on C_{60}/zeolite and K-C_{60}/zeolite. The results are shown in Figure 5. Observed DC currents on these electrodes were quite low at 298 K; however, they were enhanced under UV irradiation. The on−off response of the current on C_{60}/zeolite electrode was very sharp and quite reproducible, while the photocurrent (current under UV irradiation) of K-C_{60}/zeolite electrode was enhanced much drastically than that of C_{60}/zeolite electrode. No such current response was observed on the zeolite electrode. Therefore it is concluded that the intrazeolitic C_{60} molecules are responsible for the UV-enhanced current increases. The band gap of zeolite is extremely large and the defect sites will absorb UV photon.[37,38] The origin of the photocurrent on C_{60}/zeolite electrode will be associated with the HOMO−LUMO gap (1.9 eV) excitation of C_{60}.[39]

It is significant to determine whether the semiconductor character of C_{60}/zeolite electrode is p- or n-type. Unfortunately, neither measurement of the Hall effect nor of the Perchez effect was possible because sample settings for these measurements

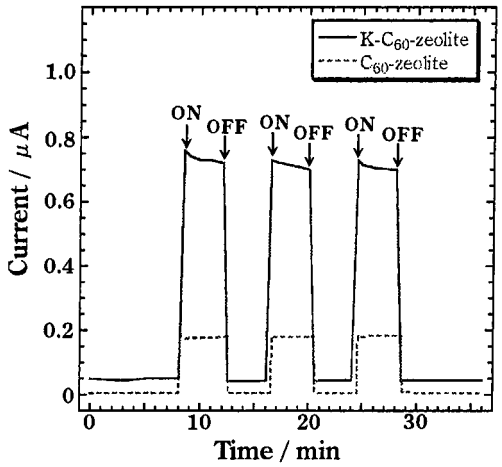

Figure 5. Current measured under dark and UV irradiation on the C_{60}/zeolite and the K-C_{60}/zeolite electrodes represented in dotted and solid lines, respectively.

were physically difficult. Therefore gas adsorption method was applied. It is well-known that oxygen gas is adsorbed as O_2^- on solid surfaces. It is based on the low electron affinity of O_2 (0.451 eV).[40] Then the electron must be supplied from the solid surface. If a n-type semiconductor is exposed to oxygen gas, the carrier electron will be lost as O_2^- and the current on the surface should decrease. The effect of O_2 adsorption on photocurrent was studied on C_{60}/zeolite electrode. The results are shown in Figure 6. When UV was irradiated on the C_{60}/zeolite electrode at 298 K, the current was enhanced repeatedly as shown in section A in Figure 6. When oxygen (24 hPa) was introduced to the C_{60}/zeolite electrode under UV irradiation, the current decreased in two ways. One was a rapid decay and the other was a slow decay with time, which are shown in section B. The sharp current drop can be interpreted as the contribution from photogenerated electrons on C_{60}/zeolite electrode captured by adsorbed oxygen. The current reached after O_2 adsorption was still higher than the dark current. The difference will be due to the contribution from photogenerated holes. Since the contribution from photogenerated electrons is larger than that of the photogenerated holes as much as 4 times, it will be possible to conclude that the C_{60}/zeolite electrode is a n-type semiconductor.

When the system was evacuated at 298 K under UV irradiation, the photocurrent increased slowly to be a constant value, which are shown in sections C and D. The value reached after evacuating the C_{60}/zeolite electrode under UV irradiation was still lower than the one measured on the fresh C_{60}/zeolite electrode under UV irradiation. When UV irradiation was stopped, the current decreased to be the same level as the starting point. It is noted that the number of photogenerated electrons decreased gradually as O_2 introduction−evacuation cycles were repeated under UV irradiation. After the cycles were repeated several times, the contribution from the slow current decay was lost, especially in section D. The diffusion of oxygen gas into zeolite pores may be responsible for the slow current decay. The interaction between O_2 and C_{60} is very weak.[41] Between O_2 and fullerene the charge transfer is very small (about 0.04e) as both electron affinity (EA) of C_{60} (2.65 eV)[42] and O_2 (0.451 eV)[40] is relatively small.[8] As expected from their EA values, electrons should transfer from O_2 to C_{60} to form $O_2^{\delta+}-C_{60}^{\delta-}$. However, the conductivity of C_{60} film is decreased as much as 4 orders of magnitude by the intercalation of O_2.[35,36,43] It has been suggested that oxygen is very effective electron traps and its intercalation into C_{60} molecules reduces the conductivity by

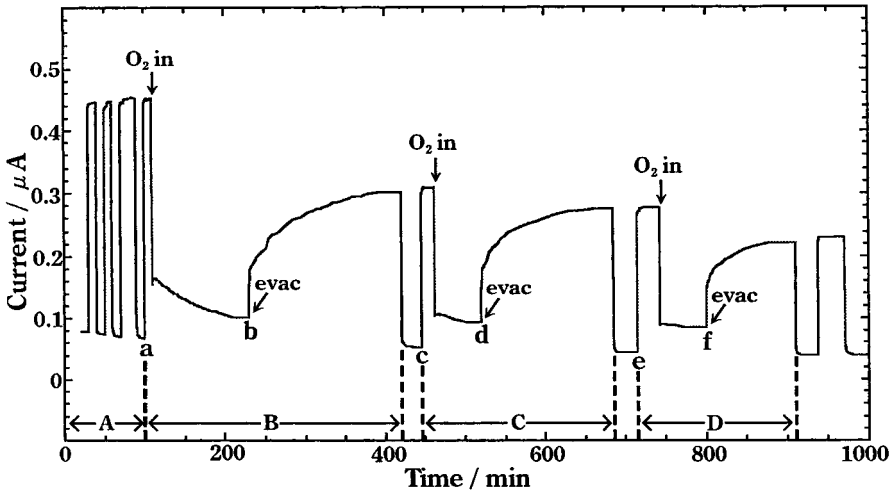

Figure 6. Oxygen introduction effects on currents measured on the C_{60}/zeolite electrode under UV irradiation. UV is repeatedly irradiated in section A. In section B, oxygen is introduced under UV irradiation and the system is evacuated in point b. Same experiments are repeated in sections C and D, where evacuation starts at point d and f. UV irradiation is ceased under vacuum at points a, c, and e.

introducing deep electronic states inside the gap.[8] The intercalation occurs in two steps: rapid quenching of electronic transport and slow diffusion through the voids of the C_{60} crystal structure.[8] The very small energy (about 30 kJ/mol)[44] to remove O_2 molecules from C_{60} film supports the diffusion process. Consequently, the slow current decay can be associated with the diffusion of O_2 into zeolite pores, in which C_{60} molecule(s) is (are) present.

Oxidation of C_{60} will be one of the reasons for the slow current decay. Since deuterium lamp was irradiated to the C_{60}/zeolite electrode through the quartz window, which should cut wavenumbers below 240 nm, no oxygen dissociation can be expected on the electrode. However, $-O-C_{60}-$ polymeric species has been suggested in the presence of O_2 at any temperature.[45] The intercalation becomes irreversible following heating C_{60} samples in the presence of O_2.[46] However, the intercalation is reversible when annealing at about 430 K under dynamic evacuation.[35,36,43,47] In our experiments, the photocurrent was rejuvenated to be more than 80% of that on the fresh C_{60}/zeolite electrode after evacuating it at 400 K overnight. The result clearly implies that the slow current decay is caused by the reversible process, that is, diffusion of oxygen into zeolite pores. Currents at points b, d, and f were almost the same value, and simultaneously, those at a, c, and e were the same. These results imply that the contribution from photogenerated electrons decreases as oxygen adsorption experiments are repeated, however, that from photogenerated holes do not change. The latter contributions will probably be attributed from zeolite electrode. Supercages in zeolite-Y are connected tetrahedrally one another so that C_{60} clusters in supercages conform a new diamond-like structure. Our work is based on this idea.

The gas sensing character of C_{60}/zeolite electrode was studied with adsorption of carbon monoxide, ammonia, and ethylene at 298 K. Current increase was observed with ethylene in the dark reaction. However, the current of C_{60}/zeolite electrode was decreased by ethylene adsorption under UV irradiation. The photocurrent decrease seemed to depend on ethylene pressure. On the contrary to this, the dark-current increase seemed to depend on ethylene pressure in the gas phase. The result is shown in Figure 7. When fresh C_{60}/zeolite electrode was exposed to ethylene as much as 9.3 hPa (7.0 Torr) at 298 K, the dark current increased abruptly from 43 to 80 pA, then decreased in two ways: one was rapid decay and the other was gradual one with time. The surface temperature should increase

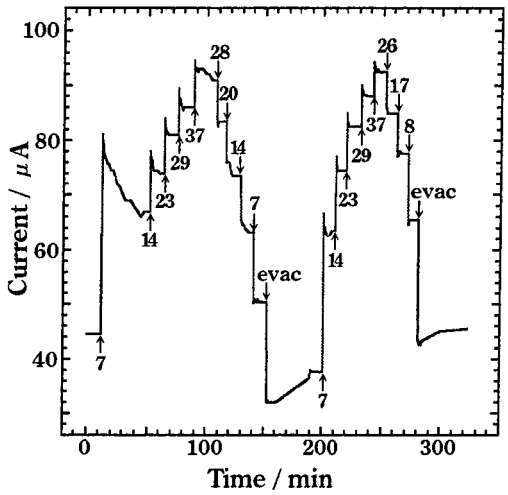

Figure 7. Dark current measured on C_{60}/zeolite electrode as a function of ethylene pressure in gas phase. Ethylene pressure is increased and then decreased in a stepwise fashion. Two such cycles are repeated. Values in the figure represent ethylene pressure in Torr scale in gas phase. Note that 1 Torr corresponds to 1.33 hPa.

because of exothermic chemical adsorption of ethylene on clean zeolite surface. The current of C_{60}/zeolite electrode should increase as temperature increases because of the semiconductor character. Thus the abrupt current rise in the first ethylene introduction will be caused by the temperature increase in ethylene adsorption on the fresh electrode. The dark current increased several times as ethylene pressure in gas phase was increased. Then the abrupt current rise and sharp current decay to reach a stabilized value are reproducible as shown in Figure 7. After ethylene was introduced to the sensing system of C_{60}/zeolite electrode to finally 49.2 hPa (37.0 Torr) in summation, the system was then evacuated to decrease ethylene pressure in gas phase. When ethylene pressure in gas phase was decreased, the dark current responded sharply to reach a stabilized value. The behavior was reproducible in each step when decreasing ethylene pressure. After evacuating the C_{60}/zeolite electrode at 298 K for 50 min, the same experiment was repeated. The increased current depended on ethylene pressure as shown in Figure 7. The rapid current overshoot was observed every time when introducing ethylene pressure. When ethylene pressure was decreased, the corresponding current dropped abruptly each

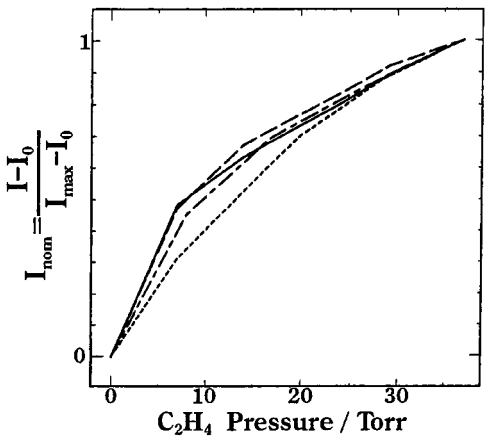

Figure 8. The dark current induced by ethylene adsorption. Values in Figure 7 are used, and currents are normalized. The value I represents an increased current at ethylene pressure in the accumulated amount, which is referenced to that under vacuum, I_0, while I_{max} is the maximum current at 49.2 hPa (37 Torr). The solid (—) and fine dotted (- -) line represent the first ethylene adsorption experiment in increasing pressure and decreasing pressure, respectively. While rough dotted (— —) and one point dotted (— -) line represent the second ethylene adsorption experiment in increasing pressure and decreasing pressure, respectively.

time. Finally it also holds true in ethylene pressure decreasing steps that the observed current seems to depend on ethylene pressure. The relation between observed current and ethylene pressure is plotted in Figure 8. The increased current, I, was an accumulated value referred to the value recorded under vacuum and the maximum current, I_{max}, was estimated as a stable current observed after introducing 49.2 hPa (37.0 Torr) ethylene in Figure 7. Of course I_0 represents the current value detected at ethylene pressure of 0 hPa measured after evacuating the C_{60}/zeolite electrode at 298 K. The values of I are, for instance, 23 (67−44) pA, 29 (73−44) pA, and 38 (82−44) pA at 9.31 (7.0), 18.62 (23.0), and 30.6 hPa (29.0 Torr) in Figure 7, respectively. The vertical scale represents Langmuir type adsorption isotherm.

It is significant to note that an abrupt current rise and the followed gradual current decay with time were observed at the first ethylene introduction in Figure 7. Of course the behavior was characteristic of the C_{60}/zeolite electrode. A dark current should rise when the surface temperature increases since the C_{60}/zeolite electrode is a semiconductor. Temperature programmed desorption experiments of ethylene were carried out on the zeolite and C_{60}/zeolite electrodes (data not shown). Desorption of ethylene started at about 333 K and showed the desorption maximum at 353−373 K. Therefore ethylene is chemically adsorbed on zeolite at 298 K. Then temperature of the zeolite surface should increase because of the heat of ethylene adsorption. It is concluded that the abrupt current rise at the first ethylene introduction in Figure 7 is due to the temperature rise induced by the heat of adsorption at 298 K. Relaxation of the heat for chemical adsorption of ethylene on zeolite will be quite slow and need time, which is responsible for the gradual current decay with time. Therefore the current increase at the first introduction of 9.31 hPa ethylene at 298 K has to be estimated as the stable one after the gradual current decay with time. Zeolite surface should have been fully covered with ethylene after the first ethylene introduction. In fact, no heat of adsorption occurred at the second ethylene introduction in Figure 7. However, the C_{60}/zeolite electrode can detect ethylene pressure in the gas phase. Then the current response in Figure 7 seems to be based on physically adsorbed ethylene, while the ethylene adsorption on the C_{60}/zeolite electrode shows a Langmuir type adsorption isotherm as shown in Figure 8. It is sufficient to make one imagine that the isotherm is reflected by a chemically adsorbed state below surface adsorption coverage of unity. The key to solve the discrepancy will be a characteristic of zeolite. As ethylene pressure in the gas phase increases, ethylene molecules can be compressed in zeolite pores. C_{60}/zeolite electrode will be able to detect such ethylene molecules. The zeolite electrode itself will probably be able to detect ethylene pressure fluctuation. However, the conductance of zeolite electrode is too low to measure. The current observed in the C_{60}/zeolite electrode will be enhanced by C_{60} in zeolite pores.

Conclusions

The semiconductor character of C_{60}/zeolite was first reported. It is based on the fact that zeolite film can be prepared as a device on electrodes for measuring currents. C_{60}/zeolite and K-C_{60}/zeolite show similar dependence of current in dark on temperature of zeolite itself. According to oxygen adsorption experiments under UV irradaiation, photogenerated carriers are mainly electrons (80%); however, there was some contribution from holes (20%). Oxygen diffusion into zeolite pores will occur slowly at 298 K and will significantly cause a slow current decay with time. Ethylene sensing can be possible under dark and obeys a Langmuir type isotherm, which will be attributed to compression of ethylene molecules into zeolite pores.

References and Notes

(1) Kroto, H. W.; Heath, J. R.; O'Brien, S. C.; Curl, R. F.; Smalley, R. E. *Nature* **1985**, *318*, 162.
(2) Hebard, A. F.; Rosseinsky, M. J.; Haddon, R. C.; Murphy, D. W.; Glarun, S. H.; Palstra, T. T. M.; Ramirez, A. P.; Kortan, A. R. *Nature* **1991**, *350*, 600.
(3) Tanigaki, K.; Ebesson, T. W.; Saito, S.; Mizuki, J.; Tsai, J. S.; Kubo, Y.; Kuroshima, S. *Nature* **1991**, *352*, 222.
(4) Kelty, S. P.; Chen, C. C.; Lieber, C. M. *Nature* **1991**, *352*, 223.
(5) Kochanski, G. P.; Hebard, A. F.; Haddon, R. C. Fiory, A. T. *Science* **1992**, *255*, 184.
(6) Xiang, X.-D.; Hou, J. G.; Crespi, V. H.; Zettl, A.; Cohen, M. L. *Nature* **1993**, *361*, 54.
(7) Stepniak, F.; Benning, P. J.; Poirier, D. M.; Weaver, J. H. *Phys. Rev. B* **1993**, *48*, 1899.
(8) Firlej, L. *Condens. Matter News* **2000**, *8*, 22.
(9) Johnson, R. D.; Meijer, G.; Bethune, D. S. *J. Am. Chem. Soc*. **1990**, *112*, 8983.
(10) Andersson, T.; Nilsson, K.; Sundahl, M.; Westman, G.; Wennerstrom, O. *J. Chem Soc., Chem. Commun*. **1992**, 604.
(11) Hetzer, M.; Bayerl, S.; Camps, X.; Vostrowsky, O.; Hirsch, A.; Bayerl, T. M. *Adv. Mater*. **1997**, *9*, 913.
(12) Braun, M.; Hirsch A. *Carbon* **2000**, *38*, 1565.
(13) Wang, Y. *J. Phys. Chem*. **1992**, *96*, 764.
(14) Silbley, S. P.; Campbell, R. L.; Silber, H. B. *J. Phys. Chem*. **1995**, *99*, 5274.
(15) Matsubara, Y.; Toda, S. G.; Yoshida, Z. *J. Org. Chem*. **1997**, 60, 5372.
(16) Silbley, S. P.; Nguyen, Y. T.; Campbell, R. L.; Silber, H. B. *Spectrochim. Acta* **1997**, *A53*, 679.
(17) Hendricks, E.; Kippelen, B.; Thayumanavan, S.; Marder, S. R.; Persoons, A.; Peyghambarian, N. *J. Chem. Phys*. **2000**, *112*, 9557.
(18) Ungurrenasu, C.; Airinei, A. *J. Med. Chem*. **2000**, *43*, 3186.
(19) Tada, T.; Kanayama, T. *Jpn. J. Appl. Phys*. **1996**, *35*, L63.
(20) Ishii, T.; Nozawa, H.; Kuramochi, E.; Tamamura, T. *Mater. Res. Soc. Symp. Proc*. **2000**, *584*, 103.
(21) Meier, W. M.; Olson, D. H. *Atlas of Zeolite Structure Types*, 3rd revised ed.; Butterworth-Heinemamm: Woburn, MA, 1992.
(22) Keizer, P. N.; Morton, J. R.; Preston, K. F.; Stugden, A. K. *J. Phys. Chem*. **1991**, *95*, 7117.
(23) Slinkin, A. A.; Emberson, S. C. Derouane, E. G. *Kinet. Catal*. **1994**, *35*, 102.
(24) Jeon, I. C.; Hong, S. B. *Bull. Korean. Chem Soc*. **1993**, *14*, 305.
(25) Anderson, M. W.; Shi, J.; Leigh, D. A.; Moody, A. E.; Wade, F. A.; Hamilton, B.; Carr, S. W. *J. Chem Soc., Chem Commun*. **1993**, 533.
(26) Hamilton, B.; Rimmer, J. S.; Anderson, M,; Leigh, D. *Adv. Mater*. **1993**, *5*, 583.

(27) Launois, P.; Moret, R.; Bolloc'h, D. Le.; Albouy, P. A.; Tang, Z. K.; Li, G.; Chen, J. *Solid State Commun*. **2000**, *116*, 99.
(28) Choo, C.-K.; Sakamoto, T.; Tanaka, K.; Nakata, R.; Asakawa, T. *Appl. Surf. Sci*. **1999**, *140*, 126.
(29) Wang, L.-S. *Chem. Phys. Lett*. **1992**, 182, 5.
(30) Whitten, T. V. Jpn. Patent, S49-24000, 1974.
(31) Saito, A.; Foley, H. C. *Microporous Mater*. **1995**, *3*, 531.
(32) Yamada, T.; Johkan, K. Okuhara, T. *Microporous Mesoporous Mater*. **1998**, *26*, 109.
(33) Schriver, D. F.; Drezdson, M. A, *The Manipulation of Air-Sensitive Compounds*, 2nd ed.; Wiley: New York, 1986.
(34) Mort, J.; Ziolo, R.; Machonkin, M.; Huffman, D. R.; Fergusson, M. I. *Chem. Phys. Lett*. **1991**, *186*, 284.
(35) Arai, T.; Murakami, Y.; Suematsu, H.; Kikuchi, K.; Achiba, Y. Ikemoto, I. *Solid State Commun*. **1992**, *84*, 827.
(36) Firley, L.; Zahab, A. *Solid State Commun*. **1993**, *87*, 893.
(37) Ishigoh, K.; Tanaka, K.; Zhuang, Q.; Nakata, R. *J. Phys. Chem*. **1995**, *99*, 12231.
(38) Tanaka, K.; Ishigoh, K.; Nakata, R. *J. Phys. Chem*. **1996**, *100*, 14074.
(39) Saito, S.; Oshiyama, A. *Phys. Rev. Lett*. **1991**, *66*, 2637.
(40) Weast, R. C. In *CRC Handbook of Chemistry and Physics*; CRC Press: West Palm Beach, FL, 1992.
(41) Kaneko, K.; Ishii, C. Arai, T.; Suematsu, M. *J. Chem. Phys*. **1993**, *97*, 6764.
(42) Wang, L.-S. *Chem. Phys. Lett*. **1992**, *182*, 5.
(43) Pevzner, B.; Hebard, A. F.; Dresselhaus, M. S. *Phys. Rev. B* **1997**, *55*, 16439.
(44) Tutt, L. W.; Boggs, T. F. *Prog. Quantum Electron*. **1993**, *17*, 299.
(45) Morris, D. E.; Singh, K. K.; Sinha, A. P. B. *J. Mater. Res*. **1993**, *8*, 2273.
(46) Dworkin, A.; Szwarc, H.; Ceolin, R. *Europhys. Lett*. **1993**, *22*, 35.
(47) Bernier, P.; Lyuk'Yanchuk, I.; Belahmer, Z.; Ribet, M.; Firley, L. *Phys. Rev. B* **1996**, *53*, 7535.